Neuroscience (2004) 124(2):467-480.

Changes in the excitability of hindlimb motoneurons during muscular atonia induced by stimulating the pedunculopontine tegmental nucleus in cats

Takakusaki, K ; Habaguchi, T ; Saitoh, K ; Kohyama, J

Ms. No. NSCI 1117, Revised version

Changes in the excitability of hindlimb motoneurons during muscular atonia induced by stimulating the pedunculopontine tegmental nucleus in cats.

Takakusaki, K., Habaguchi, T[1]., Saitoh, K. and Kohyama, J.[2]

Department of Physiology II, College of Medicine, Asahikawa Medical College, Midorigaoka Higashi 2-1, Asahikawa 078-8510, JAPAN.

Present address
1. Department of Orthopedics, College of Medicine, Asahikawa Medical College, Midorigaoka Higashi 2-1, Asahikawa 078-8510, JAPAN.
2. Department of Pediatrics, Tokyo Medical Dental University, 1-5-45 Yushima, Bunkyo-ku, Tokyo 113-0034, JAPAN.

- Abstract; 282 words
- A running title; 49 words
- Keyword; 6 words
- 8 Figures
- 1 Table

Author for correspondence
Kaoru Takakusaki, M.D. Ph.D.
Department of Physiology II, Asahikawa Medical College
Midorigaoka Higashi 2-1, Asahikawa 078-8510, JAPAN.
Tel: 011-81-166-68-2331
Fax: 011-81-166-68-2339
E-mail: kusaki@asahikawa-med.ac.jp (K. Takakusaki)

Abbreviations

A, anterior
ABSm, anterior biceps-semimembranosus
CDPs, cord dorsum potentials
CNF, cuneiform nucleus
CS, centralis superior
EDL, extesorum digitorum longus
EMGs, electromyograms
EPSPs, excitatory postsynaptic potentials
FDL, flexor digitorum longus
GABA, γ-amino butyric acid
H, horizontal
HW, half width
IC, inferior colliculus
I.R., input resistance
IS-SD, initial segment-somatodendric
IPSPs, inhibitory postsynaptic potentials
LDT, laterodorsal tegmental nucleus
LG-S, lateral gastrocnemius-soleus
LR, left and right
MG, medial gastrocnemius
MN, motoneuron
M.P., membrane potential
MRF, medullary reticular formation
NRPo, nucleus reticularis pontis oralis
PBSt, posterior biceps-semitendinosus
Pl, plantaris
P, posterior
PPN, pedunculopontine tegmental nucleus
PRF, pontine reticular formation
P, pyramidal tract
Q, quadriceps femoris
RD, raphe dorsalis
REM, rapid eye movement
SC, superior colliculus
SCP, superior cerebellar peduncle
SNr, substantia nigra pars reticulata
TA, tibialis anterior
TTP, times to peak

Keywords

- Pedunculopontine tegmental nucleus
- α-motoneurons
- Postsynaptic inhibition
- Decerebrate preparation
- Muscular tonus
- REM sleep

A Running title. Pedunculopontine inhibition of spinal motoneurons

Abstract

We have previously reported that electrical stimulation delivered to the ventral part of the pedunculopontine tegmental nucleus (PPN) produced postural atonia in acutely decerebrated cats (Takakusaki et al., Neuroscience 119, 293-308, 2003). The present study was designed to elucidate synaptic mechanisms acting on motoneurons during postural atonia induced by PPN stimulation. Intracellular recording was performed from 72 hindlimb motoneurons innervating extensor and flexor muscles, and the changes in excitability of the motoneurons following the PPN stimulation were examined. Repetitive electrical stimulation (20–50 μA, 50 Hz, 5–10 s) of the PPN hyperpolarized the membrane potentials of both the extensor and flexor motoneurons by 2.0–12 mV (6.0 $\pm$ 2.3 mV, n=72). The membrane hyperpolarization persisted for 10–20 seconds even after termination of the stimulation. During the PPN stimulation, the membrane hyperpolarization was associated with decreases in the firing capability (n=28) and input resistance (28.5 $\pm$ 6.7 %, n=14) of the motoneurons. Moreover the amplitude of Ia EPSPs was also reduced (44.1 $\pm$ 13.4 %, n=14). After the PPN stimulation, these parameters immediately returned despite that the membrane hyperpolarization persisted. Iontophoretic injections of chloride ions into the motoneurons reversed the polarity of the membrane hyperpolarization during the PPN stimulation. The polarity of the outlasting hyperpolarization however was not reversed.

These findings suggest that a postsynaptic inhibitory mechanism, which was mediated by chloride ions, was acting on hindlimb motoneurons during PPN-induced postural atonia. However the outlasting motoneuron hyperpolarization was not due to the postsynaptic inhibition but it could be due to a decrease in descending excitatory systems. The functional role of the PPN in the regulation of postural muscle tone is discussed with respect to the control of behavioral states of animals.

Postural muscle tone, which is defined by tonic muscular tension that permits standing, is completely diminished during rapid eye movement (REM) sleep. The mesopontine cholinergic neurons in the pedunculopontine tegmental nucleus (PPN) as well as the laterodorsal tegmental nucleus (LDT) are considered to be involved in the cortical desynchronization of the electroencephalogram (EEG) during REM sleep through their ascending projections to the non-specific thalamic nuclei (Datta, 2002; Datta and Siwek, 2002; Garcia-Rill, 1991; Inglis and Winn 1995; Jones, 1991; Rye et al., 1997). On the other hand, both cholinergic and non-cholinergic neurons in these nuclei are suggested to responsible for muscular atonia during REM sleep through their descending projections to the pontomedullary reticular formation (Lai et al., 1993; Mitani et al. 1988; Semba, 1993; Shiromani et al., 1990; Takakusaki et al. 1996, 2002). Experiments using intracellular recordings in chronic cats have revealed that the excitability of α-motoneurons innervating hindlimb muscles is profoundly depressed during REM sleep (Glenn and Demment, 1981a, 1981b; Morales and Chase 1978).

Postural muscle tone is well developed in acute decerebrate animals due to decerebrate rigidity, and the decerebrate preparation has been utilized for understanding the mechanisms of controlling postural muscle tone (Morales et al., 1987; Mori, 1987). The dorsomedial part of the pontine reticular formation (PRF) is referred as pontine inhibitory area (PIA) where injections of cholinergic agents lead to induction of muscular atonia in not only intact (Katayama et al., 1984; Vannie-Mercier et al., 1989; Yamamoto et al., 1990) but also decerebrate (Morales et al., 1987; Takakusaki et al., 1993, 1994) animals. In addition, medial part of the medullary reticular formation (MRF) is called as medullary inhibitory region, where either electrical (Magoun and Rhines, 1946; Habaguchi et al., 2002; Jankowska et al., 1968, Llinás and Terzuolo, 1964, 1965; Takakusaki et al., 1994, 2001) or chemical stimulation also produced muscular atonia in decerebrate (Lai and Siegel, 1988) and intact (Chase et al., 1986; Fung et al., 1982) animals. These results suggest that a pontomedullary reticulospinal inhibitory

system mediates muscular atonia. The inhibitory system could act either directly, or via spinal inhibitory interneurons (Chase and Morales, 1990).

It has been demonstrated that an activation of PPN neurons by either electrical stimulation (Lai et al., 1990; Takakusaki et al., 2003) or microinjections of neuroactive substances (Takakusaki et al., 2003) in decerebrate preparations resulted in suppression of the postural muscle tone. The PPN projects to the PIA (Mitani et al., 1988; Lai et al., 1993; Semba K, 1993; Takakusaki et al., 1996) and to the medullary inhibitory region (MRF; Shiromani et al., 1990). It can be proposed therefore, that the PPN-induced muscle tone suppression is produced by activation of the PPN neurons projecting to these reticular formation areas. In the present study, attempts have been made to elucidate the synaptic effects acting on motoneurons during the PPN-induced motor inhibition. For this purpose intracellular recordings were performed from hindlimb motoneurons in acutely decerebrate cats so that we could examine the changes in the electrophysiological properties of motoneuron membranes induced by electrical stimulation of the PPN. In particular, we substantiated whether changes in the excitability of motoneurons following the PPN stimulation were equivalent to those induced by stimulation of the medullary inhibitory region (Habaguchi et al., 2002; Jankowska et al., 1968, Llinás and Terzuolo, 1964, 1965) and to those observed during REM sleep in intact animals (Glenn and Dement, 1981a, b, c; Morales and Chase, 1978). The functional role of the PPN in the regulation of postural muscle tone is discussed with respect to the control of behavioral states of animals. A preliminary report has been published elsewhere (Takakusaki et al., 1997a).

Experimental procedures

All the procedures of the present experiments were approved by the Animal Studies Committee of Asahikawa Medical College and are in accordance with the Guide for the Care and Use of Laboratory Animals (NIH Guide), revised 1996. Every attempt was made to minimize animal suffering and to reduce the number of animals used. The study is based on the data from 14 adult cats (raised in an animal laboratory of Asahikawa Medical College) of either sex which weighed from 2.6 to 4.1 kg.

Surgical procedures.

The trachea of each cat was intubated after the animal was anesthetized with halothane (Flothane, Takeda Co., Osaka, Japan) (0.5–3.0%) and nitrous oxide gas (0.5–1.0 l/min) with oxygen (3.0–5.0 l/min). A cannula was placed in the femoral artery to monitor the blood pressure and in the cephalic vein for administration of pancronium bromide (Myoblock, Sankyo Co., Tokyo, Japan) (0.1 mg/kg). A laminectomy was performed to expose the lumbosacral segments (L4–S1). The animals were surgically decerebrated at the precollicular-postmammillary level, and the anesthesia was then discontinued. The head and the vertebrae of the lumbar segments of each animal were fixed in a stereotaxic apparatus. The rigid spinal frame securely held an animal by pins in the iliac crests, clamps on the dorsal processes of L1–3, and a clamp on the vertebral body of L7. Retraction of the skin permitted the formation of a wall for a pool of oil which covered the exposed cervical and/or lumbosacral cord.

After the surgery, the cat was allowed to assume a reflex standing posture which was due to the decerebrate rigidity. Repetitive stimuli were then delivered to the mesopontine tegmentum so that the optimal stimulus site for producing a collapse of the decerebrate rigidity could be determined (see Takakusaki et al., 2003). Following this procedure the cats were again anesthetized for further surgery. Two AgCl wires, 0.3 mm diameter and separated by a distance of 2 mm, were used as electrodes for the

stimulation of the left hindlimb nerves which were dissected. The names and abbreviations of the left hindlimb nerves which were dissected and mounted on the bipolar electrodes are as follows: posterior biceps-semitendinosus (PBSt), anterior biceps-semimembranosus (ABSm), quadriceps femoris (Q), lateral gastrocnemius-soleus (LG-S), medial gastrocnemius (MG), tibialis anterior (TA), extesorum digitorum longus (EDL), flexorum digitorum longus (FDL), and plantaris (Pl). In 4 cats, the ventral roots from L6, L7, and S1, were completely dissected so that either orthodromic spikes (Fig.4), Ia EPSPs (Fig.7), or Ia IPSPs (Fig.8) could be induced. In these animals, the L6, L7, and S1 ventral roots were cut, and their central ends were mounted on bipolar electrodes which served as stimulation electrodes. In 3 cats, the dorsal roots from L5 to S1 were dissected so that the firing capability of antidromic spikes following the PPN stimulation could be determined (Fig.4B).

Throughout an experiment the temperature of the animal's rectum and the oil pool was monitored and maintained at 36–37 ^{o}C by using radiant heat lamps. The end tidal CO_2 was maintained between 4 and 6%. The cats were immobilized by an infusion of pancronium bromide and were artificially respired during the intracellular recording. The mean blood pressure was maintained at more than 100 mmHg.

Stimulation, recording and data analyses.

The stimulating electrode, which was a glass micropipette with a carbon fiber and a Woods metal tip (diameter 7 μm, resistance 0.2–0.5 MΩ; Takakusaki et al., 2003) was inserted into the mesopontine tegmentum (anterior (A) 1.0 to posterior (P) 3.0, left and right (LR) 2.0 to 5.0, horizontal (H) +2.0 to -7.0). To examine the mesencephalic stimulus effects on muscle tone, repetitive stimuli (20–50 μA, 0.2 ms duration, and a frequency of 50 Hz) were delivered for 5 to 10 seconds. The mesopontine tegmentum was then stimulated at 0.5–1.0 mm intervals in the dorsoventral, mediolateral and rostrocaudal directions. Electromyograms (EMGs) were bilaterally recorded from the

soleus muscles with thin, bipolar, stainless steel wires.

During intracellular recording, repetitive stimuli (20–50 μA, 0.2 ms duration, and a frequency of 50 Hz) were delivered for 5 to 10 seconds to the optimal stimulus site in the PPN. The effects on motoneurons were further studied by moving the electrode in 0.5–1.0 mm intervals in the dorsoventral, mediolateral and rostrocaudal directions (Fig.2). Intracellular recordings were obtained from both extensor and flexor motoneurons located at the L6–S1 segments. A glassmicropipette filled with 2 M K-citrate or 3 M KCl (tip diameter 1.0–1.5 μm, impedance 5–10 MΩ) was used as a recording electrode. The electrode was connected to a high input impedance preamplifier with negative capacitance compensation (Neurodata model IR 184, Cygnus Tech, Pennsylvania, USA). A reference electrode was placed in the temporal muscles.

Fifty-eight α-motoneurons were identified by antidromic invasion from peripheral muscle nerves (Fig.1Cb; Habaguchi et al., 2002; Takakusaki et al., 1993a). Fourteen α-motoneurons were antidromically identified by stimulating ventral roots. These 14 motoneurons were classified according to the pattern of monosynaptic EPSPs from group Ia fibers (Eccles and Lundberg, 1958; Takakusaki et al., 2001). They were analyzed only if their antidromic action potentials and membrane potentials exceeded 60 mV (mean 68.2±3.7 mV, n=72) and -50 mV (mean –60.7±4.2 mV, n=72), respectively. The membrane potential of each motoneuron was monitored with a low gain DC display. The mean membrane potential was measured by drawing an isopotential line through a polygraph tracing so that it bisected the synaptic noise (Glenn and Dement, 1981a; Takakusaki et al., 1993a). In firing cells, a threshold membrane potential for generating action potentials was used as the membrane potential. The antidromic or orthodromic spikes were induced by stimulating individual nerves with rectangular pulses (0.2 ms duration) delivered at a frequency of 1 Hz (Fig. 4A and B). Constant-current pulses of 5–30 nA with a duration of 100–200 μs were passed through the microelectrode at intervals of 1–2 s for evoking direct spikes (Fig. 4C).

Anodal or anodal-cathodal current pulses of 40–50 ms duration with an intensity of 5-10 nA were also injected intracellularly to estimate the input resistance in the absence of anomalous rectification (Glenn and Dement, 1981b; Takakusaki et al., 1993a, Habaguchi et al., 2002) (Fig.5). The input resistance was calculated from the voltage shift in response to the anodal-cathodal current pulses. A glass micropipette filled with 3 M KCl was used to inject chloride ions into the recorded motoneuron in order to examine whether the PPN-induced effects were mediated by chloride ions (Fig.8).

Hindlimb muscle nerves were also stimulated to record either Ia EPSPs (Fig.7) or Ia IPSPs (Fig.8). A signal processor (Model 7T07A, Sanei Co., Tokyo, Japan) was used to average the Ia EPSPs (usually 10–20 sweeps) so that the parameters of the shape of the EPSP could be accurately measured (Table 1). Cord dorsum potentials (CDPs) were recorded by means of a platinum ball electrode placed on the dorsal root entry zone of the rostral L7 segment against an indifferential electrode placed in the back muscles. These recordings were used for monitoring the incoming volley from the peripheral nerves. The recordings monitored the amplitude of the stimuli, expressed in multiples of the threshold strengths (xT), which were applied to the peripheral nerves. The individual peripheral nerves were stimulated every second using single rectangular pulses with a stimulus intensity of less than 1 mA and a duration of 0.2 ms. All the records were displayed on a storage oscilloscope and stored for later analysis on magnetic tape (FM recorder, Model LX 10, TEAC inst. Kanagawa, Japan; bandwidth 0–10.0 kHz).

Histological controls and ChAT immunohistochemistry

At the end of each experiment the stimulus sites were marked with electrolytic microlesions which were produced by passing a DC current of 30 μA for 30 seconds through the stimulating electrode. Animals (n=8) were then sacrificed by an overdose of Nembutal anesthesia, and the brainstem was removed and fixed in 10 % formalin in

saline. Later, frozen 50 μm frontal sections or parasagittal sections were cut and stained with cresyl violet. The locations of the microlesions were identified with reference to the stereotaxic atlases of Berman (1968) and Snider and Niemer (1961).

Choline acetyltransferase (ChAT) immunohistochemistry was performed to identify the boundaries of the PPN so that we could elucidate whether the effective stimulus sites were located within the PPN. After the experiments, 6 animals were deeply anaesthetized with Nembutal and transcardially perfused with 0.9 % saline followed by a solution of 3.0 % paraformaldehyde (0.01%) glutaraldehyde in 0.1 M phosphate buffer (pH 7.4). The brain of each cat was removed, saturated with a cold solution of 30 % sucrose, and 50 μm frozen sections were prepared. ChAT immunohistochemistry was then performed by using the peroxidase-antiperoxidase method combined with diaminobenzidine (Lai et al., 1993; Mitani et al., 1988; Takakusaki et al., 2003). Monoclonal anti-ChAT antibody (Boehringer Mannheim, Germany) was used for these preparations.

Results

Identification of effective stimulus sites in the PPN for the inhibition of motoneurons

An effective muscle tone inhibitory region in the mesopontine tegmentum was first identified. Figure 1A shows an example of the optimal stimulus site which was marked by an electrolytic microlesion together with distribution of cholinergic neurons which were labeled by ChAT immunohistochemistry. The PPN was defined by loosely arranged cholinergic neurons that surrounded the superior cerebellar peduncle (SCP). In this animal, the electrolytic microlesion was located at the ventrolateral edge of the PPN. The distribution of the effective sites in 14 animals is shown on the representative coronal (B) and parasagittal (C) planes of the brainstem. These were mainly located in the ventral part of the PPN as previously described (Takakusaki et al., 2003).

The effects of stimulating the inhibitory region in the PPN upon the intracellular activities of 72 hindlimb motoneurons were examined. Representative recordings obtained from an LG-S motoneuron are illustrated in Fig.2. The LG-S motoneuron had a spontaneous firing with a frequency of 10 - 15 Hz. When repetitive stimuli were delivered to the inhibitory region in the PPN, which corresponds to “c” in Fig.2B, tonic firing of the motoneuron ceased and the membrane potential was hyperpolarization by 10 mV (Fig.2Ac). The membrane hyperpolarization lasted for more than 10 seconds even after termination of the stimulation. On the other hand, stimulating 2 mm dorsal to the inhibitory region depolarized the membrane potential and then produced sequences of membrane depolarization and hyperpolarization (fictive locomotion) with a cycle time of approximately 1 second (Fig.2Aa). The stimulus site corresponded to the cuneiform nucleus (CNF) (Fig.2Ba). Stimulating between these two sites (Fig.2Bb), membrane hyperpolarization which were associated with rhythmic membrane oscillations, was induced (Fig.2Ab). The cycle time of the membrane oscillations was shorter than that induced by stimulation of the CNF (Fig. 2Aa). In all animals (n=14) stimulation of the muscle tone inhibitory region in the PPN induced

membrane hyperpolarization which lasted even after termination of the stimulation in any type of motoneuron.

Changes in membrane properties of hindlimb motoneurons

Changes in membrane potentials

The intracellular recordings illustrated in Fig.3A–C were obtained from the same animal. In an LG-S motoneuron, PPN stimulation with a stimulus intensity of 30 μA ceased its spontaneous firing and gradually hyperpolarized the membrane potential by 8 mV (Fig.3Aa). By increasing the stimulation intensity (40 μA), the spontaneous firing was immediately diminished and the membrane potential was hyperpolarized by 11 mV (Fig.3Ab). Stimulation of the same PPN area also hyperpolarized the membrane potentials of Q and PBSt motoneurons, both of which had no spontaneous firing (Fig.3B and C). As shown in Fig.3D, PPN stimulation hyperpolarized every type of hindlimb motoneuron by 2–12 mV (mean $\pm$ S.D.; 6.3 $\pm$ 2.3 mV, n=72). The membrane hyperpolarization was larger in motoneurons having spontaneous firing before PPN stimulation (10 $\pm$ 1.5 mV, n=12) than in silent motoneurons (5.3 $\pm$ 1.6 mV, n=60).
It was also observed that there was a significant relationship between the degree of hyperpolarization and the prestimulus membrane potential level (Fig.3E).

Changes in firing capabilities of motoneurons

Membrane hyperpolarization alone is not conclusive evidence of a decreasing excitability of motoneurons: variations in the discharge threshold or membrane conductance could override the membrane hyperpolarization. We therefore examined the changes in the capability of action potentials. The results are shown in Fig.4. In each motoneuron, left panel shows changes in membrane potentials following PPN stimulation (30 μA and 50 μA). Right panel shows the changes in firing property of the motoneuron. Before PPN stimulation, stimulus strength applied to each muscle nerve was adjusted to induce either orthodromic (Fig. 4Aa) or antidromic (Fig. 4Ba) spikes in

each motoneuron for a firing capability of more than 0.9.

In an LG-S motoneuron (Fig. 4A), stimulation of the PPN with a stimulus intensity of 30 μA reduced the firing capability of generating orthodromic spikes along with membrane hyperpolarization (Fig. 4Ab). The generation of the orthodromic spikes was completely blocked by increasing the stimulus intensity (50 μA, Fig. 4Ac). The firing capability gradually recovered after the PPN stimulation ceased (Fig. 4Ad). Essentially the same findings were obtained from another 8 motoneurons.

In the PBSt motoneuron (Fig. 4B), stimulation of the PPN with an intensity of 30 μA increased a fragmentation of the initial segment-somatodendric (IS-SD) spikes (IS-SD delay) of the antidromic spikes (indicated by arrows) together with a membrane hyperpolarization (Fig. 4Bb). Stronger stimuli (50 μA) finally suppressed the propagation of the SD spikes (IS-SD block, Fig. 4Bc). Both the IS-SD delay and IS-SD block were not observed after the PPN stimulation and the generation of antidromic spikes gradually returned (Fig. 4Bd). Similar results were obtained in another 10 motoneurons, i.e., the beginning of IS-SD fragmentation was coincident with the development of membrane hyperpolarization. In addition, as stronger stimuli were applied the faster the IS-SD block tended to occur.

The third measure of excitability, the response to constant-current depolarizing pulses, was the final means of demonstrating an excitability drop during PPN stimulation. In 8 motoneurons, constant-current pulses of 5–30 nA with a duration of 100–200 μs were passed through the microelectrode at intervals of 1–2 s. The strength and duration were adjusted in each motoneuron for a firing capability of more than 0.9 (Fig. 4Ca). Although membrane potential was hyperpolarized, the firing capability was not decreased by weak stimuli (30 μA; Fig. 4Cb). However, stronger stimuli (50 μA) greatly reduced the firing capability (Fig. 4Cc). The firing capability gradually returned after the stimulation ceased (Fig. 4Cd).

Input resistance

Changes in the input resistance following PPN stimulation were examined in 14 motoneurons. The results are shown in Fig.5 and Table 1A. The input resistance was calculated from the voltage shift in response to the anodal-cathodal current pulses. The PBSt motoneuron shown in Fig.5A had a membrane potential of -67 mV and an input resistance of about 1.5 MΩ. (Fig.5Aa and Ba). During PPN stimulation the input resistance decreased to 1.0–1.1 MΩ (Fig.5Bb) together with a membrane hyperpolarization (Fig.5Ab). After the stimulation the input resistance was restored (Fig.5Bc), while the membrane potential did not return to the prestimulus level (Fig.5Ac). The time course of the changes in both the input resistance and the membrane potential of this motoneuron and another motoneuron (a Q-motoneuron) is shown in Fig.5Ca and Fig.5Cb, respectively. During PPN stimulation, a membrane hyperpolarization was consistently accompanied by a decrease in input resistance. After termination of the stimulation, the membrane potential did not promptly return to the prestimulus level whereas the input resistance was immediately re-established to its prestimulus level. As can be seen in Table 1A, the input resistance of 14 motoneurons was reduced to 71.5% on average, and associated with a membrane hyperpolarization of 6 mV.

Cell size and inhibition

In the present study, there is an inverse correlation between input resistance and conduction velocity in motoneurons as can be seen in Fig.6Aa. The correlation was presumably arises because both the axon diameter and input resistance have a mutual dependence on cell size (Burke 1968; Kernel, 1966; Kernel and Zwaagstra; 1981). In addition, the input resistance of the motoneurons was correlated with the membrane potential (Fig.6Ab), indicating that the excitability of the small motoneurons was higher than that of the large motoneurons. It was observed that the degree of membrane hyperpolarization which was induced by PPN stimulation was inversely correlated with the conduction velocity (Fig.6Ba). Because the degree of hyperpolarization was

correlated with a decreased input resistance (Fig.6Bb), the PPN stimulation could more strongly inhibited the excitability of the small motoneurons than the large motoneurons.

Changes in Ia EPSPs

Changes in Ia EPSPs following PPN stimulation were examined in 14 motoneurons (Fig.7 and Table 1C). Representative examples obtained from MG and PBSt motoneurons are illustrated in Fig.7A and Fig.7B, respectively. During PPN stimulation, each Ia EPSP was greatly reduced in size. The amplitude was reduced from 4.8 mV to 1.4 mV (29.2% of the control, Fig.7Ab) in an MG motoneuron, and from 6.2 mV to 1.5 mV (24.2% of the control, Fig.7Bb) in a PBSt motoneuron. The size of the amplitude of each EPSP either returned, or was increased after the PPN stimulation (Fig.7Ac and Bc, Table 1B). It should be noted that, despite the large reduction of the Ia EPSPs, the input resistance of the PBSt motoneuron was only reduced from 0.93 MΩ to 0.61 MΩ (65.6% of the control) during the PPN stimulation (lower traces in Fig.7B). The plot of the time course of the decay phase of each Ia EPSP (Fig.7Ca and Cb) illustrates that the rate of decay of the EPSP during the PPN stimulation was faster than that before, and after, the PPN stimulation. The changes in shape parameters of 14 motoneurons are summarized in Table 1B. The mean reduction of the EPSP amplitude was 43.1 %. The shape parameters such as the time to peak (TTP) and half width (HW) of the Ia EPSPs were also reduced by 24.7% and 29.6%, respectively.

Intracellular injections of chloride ions

Because the chloride-ion mediated postsynaptic inhibition was involved in membrane hyperpolarization of limb motoneurons induced by stimulating the MRF (Habaguchi et al., 2002; Jankowska et al., 1968, Llinás and Terzuolo, 1964, 1965), we finally elucidated whether the PPN-induced membrane hyperpolarization was mediated by chloride ions. For this, chloride ions were iontophoretically injected into the motoneurons and the effects of PPN stimulation upon the motoneurons were examined. Representative results are shown in Fig.8. Before injection of chloride ions, stimulating

a Ia afferent from the TA muscles induced Ia IPSPs in an LG-S motoneuron (Fig.8Aa). In the same motoneuron PPN stimulation caused cessation of spontaneous firing and hyperpolarized membrane potentials (Fig.8Ba). We then injected chloride ions. Approximately 20 minutes after the injections of the chloride ions, the Ia IPSPs was greatly reduced in size (Fig.8Ab), and membrane hyperpolarization was not induced during PPN stimulation (Fig.8Bb). After 35 minutes, the polarity of the Ia EPSPs was eventually reversed (Fig.8Ac). Stimulation of the PPN then depolarized the membrane (Fig.8Bc). However the membrane potentials gradually hyperpolarized after termination of the stimulation (Fig.8Bb and 8Bc). In 3 motoneurons (Q, PBSt and LG-S motoneurons), the changes in both the Ia IPSPs and the PPN effects following the injection of chloride ions were compared. As shown in Fig.8C, injection of chloride ions reversed the polarity of both the Ia IPSPs and the PPN-induced membrane hyperpolarization in each motoneuron. In the other 2 motoneurons (PBSt and FDL motoneurons), intracellular injections of chloride ions also reversed the polarity of PPN-induced membrane hyperpolarization. These findings suggest that the postsynaptic inhibition, which is mediated by an inward current of chloride ions, causes the membrane hyperpolarization during PPN stimulation. However, the outlasting hyperpolarization after the PPN stimulation may not be due to the postsynaptic inhibition.

Discussion

Here we provided evidence that PPN-induced muscle tone suppression was ascribed to postsynaptic inhibitory effects upon spinal motoneurons which were mediated by an inward current of chloride ions. The present results are discussed in relation to the neuronal mechanisms of a generalized motor inhibition during REM sleep. Finally, the functional role of the PPN in the state-dependent motor control will be considered.

Consideration of the stimulus effects induced by PPN stimulation

Numerous ascending and descending fibers are intermingled with cholinergic (Armstrong et al., 1983; Rye et al., 1987; Span and Grofova, 1992) and non-cholinergic neurons in the PPN area. The latter include glutamatergic (Clements et al., 1991), γ-amino butyric acid (GABAergic; Kosaka et al., 1988; Ottersen and Storm-Mathisen, 1984), and peptidergic (e.g., Substance P; Vincent et al., 1983) neurons. The PPN has been first considered as a functional region involved in the initiation of locomotion on the basis of its connections with limbic structures and the basal ganglia (Armstrong, 1986; Grillner et al., 1997; Garcia-Rill, 1991; Mogenson et al., 1993). Garcia-Rill and his co-workers (Garcia-Rill et al., 1987; Skinner et al., 1997) used ChAT immuno-histochemistry and nicotinamide adenine dinucleotide phosphate diaphorase histochemistry, and convincingly suggested that an activation of cholinergic neurons in the PPN was required to initiate locomotion. In addition, it has been suggested that the PPN is also involved in suppression of neck (Lai and Siegel, 1990) and limb muscle activities (Takakusaki et al., 2003).

Garcia-Rill et al. (1996) demonstrated that the parameters of PPN stimulation were critical for evoking either locomotion or muscular atonia; a slowly-ramped low frequency (< 50 Hz) stimulation of the PPN recruited locomotion, while a sudden onset of high-frequency (100 Hz) stimulation of the same site abolished muscle tone (Garcia-

Rill et al., 1996). From these results, they suggested that instantaneous onset of stimulation might lead to an arousal response through a paroxysmal activation of cholinergic arm of the ascending reticular activating system and induce a startle-like decrease in the level of muscle tone via descending inhibitory pathways (Garcia-Rill et al., 1996; Reese et al., 1995). In this study, we did not change stimulus parameters. Therefore we have to consider the limitation of our experimental designs.

On the other hand, we demonstrated a functional topography in the lateral part of the mesopontine tegmentum in the control of locomotion and muscle tone; optimal sites for muscular atonia were located in the ventral part of the PPN, while those for locomotion were mainly located in the CNF (Takakusaki et al., 2003). Stimuli applied between the two regions induced a mixture of muscle tone suppression and locomotion. Essentially the same results were observed in Fig.2. This figure further provided important information. Signals from the CNF induced membrane depolarization which was followed by slow membrane oscillations, while those from the dorsal PPN first hyperpolarized the membrane and generated fast oscillations. We propose that the mesopontine tegmentum including the CNF and the PPN is critical for generating diverse patterns of rhythmic movements which are produced by the integration of various cycle times and different levels of muscle tone.

Brainstem-spinal cord mechanisms of motor inhibition induced by PPN stimulation

We have shown that not only electrical stimulation but also microinjections of either glutamatergic agonists or $GABA_A$ antagonists into the ventral PPN induced muscular atonia (Takakusaki et al., 2003). Moreover, injections of atropine sulfate into the PIA (see introduction), where both cholinergic and non-cholinergic fibers from the PPN projected (Mitani et al., 1988; Lai et al., 1993; Moon-Edley and Graybiel, 1983; Semba K, 1993), attenuated the PPN-effect (Takakusaki et al., 2003). Thus the PPN stimulus effects observed in this study can be induced by an activation of PPN

cholinergic neurons projecting to the PIA. Moreover, because stimulation of the medial aspect of the PPN, such as a site “c” in Fig.2, also induced the inhibitory effects, the stimulation would be also expected to activate PPN fibers funneling toward to the PIA.

In decerebrate preparation, an injection of carbachol in to the PIA induced muscular atonia which was associated with an increase in the firing rate of a group of medullary reticulospinal neurons (Takakusaki et al., 1994). A spike-triggered averaging study revealed that the reticulospinal neurons exerted postsynaptic inhibitory effects upon motoneurons via inhibitory interneurons (Takakusaki et al., 1994). We consider that PPN stimulation excites cholinoceptive neurons in the PIA which, in turn, activate the medullary reticulospinal neurons and induce muscular atonia. On the other hand, Lai and Siegel (1988) demonstrated that an injection of either glutamatergic or cholinergic agents into the ventromedial part of the MRF suppressed postural muscle tone in cats. Since the PPN also project to the ventromedial MRF (Lai et al., 1993; Shiromani et al., 1990), both glutamatergic and cholinergic PPN neurons may also induce muscular atonia (Sakai and Koyama, 1996) through their projections to the ventromedial MRF.

Descending monoaminergic systems such as the coerulospinal and the raphespinal tracts are muscle tone facilitatory systems (Fung and Barnes, 1981; Lai et al., 2001; Sakai et al., 2000). Serotonin excites motoneurons and increases input resistance of the motoneurons in vivo (White and Fung, 1989) and in vitro (Talley et al., 1997). There are serotonergic projections to the PPN (Honda and Semba, 1994) and to the medial PRF (Semba and Fibiger, 1992); the former possibly inhibits cholinergic neurons (Leonald and Llinás, 1994), and the latter may reduce the activity of the reticulospinal inhibitory system (Takakusaki et al., 1994). Lai et al. (2001) reported that monoamine (norepinephrine and serotonin) release in the spinal cord was reduced during muscular atonia which was induced by either electrical or chemical stimulation of the PIA. They indicated that activities of the coerulospinal and raphespinal tracts were inhibited by connections from the PIA to the locus coeruleus (Sugaya et al., 1988)

and the raphe nuclei (Carlton et al., 1983; Gallager and Pert, 1978). Therefore, muscle tone can be regulated by a counterbalance between the inhibitory and the facilitatory systems. Consequently, the decrease in excitability of motoneurons following the PPN stimulation might also be due partially to the withdrawal of descending monoaminergic facilitatory systems.

Synaptic mechanisms acting on hindlimb motoneurons of PPN-induced atonia

During PPN stimulation, motoneuron hyperpolarization was associating with decreases in input resistance, firing capability and amplitude of Ia EPSPs. The reduction of the Ia EPSP was accompanied by faster decay of its declining phase and decreases in TTP and HW. All these findings indicate that postsynaptic inhibitory mechanisms are acting on motoneurons during PPN stimulation. Moreover the polarity of both the membrane hyperpolarization and Ia IPSPs was equally reversed by injecting chloride ions. Because inhibitory effects from reciprocal Ia interneurons are generated on soma of motoneurons (Jankowska and Roberts, 1972), an inward current of chloride ions can mediate the postsynaptic inhibition, which is preferentially exerted on the soma rather than distal dendrites of motoneurons. Possibly a presynaptic inhibitory mechanism is also operating during the PPN stimulation. This possibility is based on the finding that the reduction of the amplitude of the Ia EPSPs was larger than that of the somatic input resistance during the PPN stimulation. Because Ia afferents terminate on the distal dendrites of motoneurons (Mendell and Henneman, 1971), the prominent reduction of the Ia EPSPs may also be ascribed to the decrease in the excitability of Ia afferent terminals by the presynaptic inhibition.

Stimulation of the MRF induced postsynaptic inhibition of limb motoneurons in decerebrate cats (Habaguchi et al., 2002; Jankowska et al., 1968; Llinás and Terzuolo, 1964, 1965; Takakusaki et al., 2001). Habaguchi et al. (2002) demonstrated that the MRF stimulation hyperpolarized motoneurons by 5.4 mV and was associated with a

decrease in input resistance of 38%. These changes are almost equivalent to those induced by PPN stimulation in this study, i.e., PPN stimulation hyperpolarized motoneurons by 6.0 mV and reduced the input resistance by 35.5 %. It should be noted that the decrease in motoneuronal excitability during the PPN stimulation is also equivalent to that during REM sleep. In the transition from non-REM sleep to REM sleep, hindlimb motoneurons hyperpolarized by about 6 mV and the median decrease of input resistance was 39% (Glenn and Dement, 1981a, 1981b). Because PPN neurons are active during REM sleep (Koyama and Sakai, 2000; Sakai and Koyama, 1996; Steriade et al., 1990a, 1990b), motor inhibition induced by the PPN stimulation can be due to the activation of the pontomedullary inhibitory system that operates during REM sleep.

Despite the recovery of the input resistance, the membrane hyperpolarization of motoneurons continued even after termination of the PPN stimulation. One of explanations is that the persisting hyperpolarization is due to postsynaptic inhibition acting on the distal dendrites of the motoneurons which may not be detected by input resistance measurements. However, this can be disregarded, because the amplitude of the Ia EPSPs recovered after the PPN stimulation. We rather consider that a decrease in excitatory input to the motoneurons, i.e., disfacilitation possibly induces the outlasting hyperpolarization. Since a stretch reflex loop was functionally disconnected by the immobilization, a withdrawal of descending monoaminergic facilitatory systems would mediate this process. Concerning to this, Homma et al., (2002) showed an important finding that PPN stimulation induced prolonged responses in PRF neurons in vitro rat slice preparation. They postulated, if the PRF neurons were local inhibitory interneurons, the prolong effects from the PRF could reduce the excitability of reticulospinal neurons (Homma et al., 2002). It is possible that the prolong effects may also reduce the excitability of coerulospinal and raphespinal neurons during and after PPN stimulation through their connections with locus coeruleus (Sugaya et al., 1988) and raphe nuclei (Carlton et al., 1983; Gallager and Pert, 1978), resulting in disfacilitation of these

descending systems. Alternative explanation is that an intrinsic membrane property of motoneurons is involved in the outlasting hyperpolarization. In decerebrate cats, a depolarization plateau was induced in motoneurons by a brief depolarizing pulse (Crone et al., 1988). This was terminated by either a hyperpolarizing current or a short train of inhibitory synaptic inputs (Hounsgaard et al., 1984). Because the depolarizing plateau was induced after reduction of a chloride-ion conductance (Katz and Miledi, 1963; Schwindt and Crill, 1980), PPN stimulation might increase an intracellular concentration of chloride ions so that it terminated the depolarizing state and hyperpolarized the motoneurons.

A degree of the PPN-induced membrane hyperpolarization was inversely correlated with the conduction velocity of motoneurons. Because both the input conductance (an inverse of input resistance) and the conduction velocity are generally correlated with the size of the motoneurons (Burke, 1968; Kernel, 1966; Kernel and Zwaagstra, 1981), the inhibitory effects may be preferentially exerted on the small motoneurons more than on large motoneurons. Motoneuron input resistance has often been used to explain recruitment order during graded motoneuron excitation (Henneman et al., 1965; Kernell and Zwaagstra, 1981). The present findings may thus conform to the principle of recruitment according to motoneuron size (Henneman et al., 1965) if a de-recruitment by the inhibitory system is included in the principle.

Role of PPN neurons in the control of motor behavior in awake-sleep cycles

Because PPN neurons discharge not only during REM sleep but also during wakefulness (Koyama and Sakai, 2000; Sakai and Koyama, 1996; Steriade et al., 1990a, 1990b), the PPN can be involved in the expression of a variety of motor behaviors during both REM sleep and wakefulness. During REM sleep, ascending cholinergic PPN projections into the thalamus, including the lateral geniculate nucleus, possibly provide ponto-geniculo-occipital waves and EEG desynchronization (McCormick and

Bal, 1997; Steriade, 2001). Descending projections to the pontomedullary reticular formation (Lai et al., 1993; Mitani et al., 1988; Shiromani et al., 1990; Takakusaki et al., 1996) are thought to mediate muscular atonia via the reticulospinal tract (Chase and Morales, 1990; Takakusaki et al., 1994). On the other hand, during wakefulness, changes in the activity of PPN neurons preceded the onset of arm movements (Matsumura et al., 1997). Moreover an injection of muscimol, a $GABA_A$ agonist, into the PPN reduced the speed of arm movements and delayed the onset of movements (Matsumura and Kojima, 2001). The PPN may thus facilitate the voluntary limb movements through its excitatory connections with dopaminergic neurons in the substantia nigra (Kojima et al., 1997). In addition, the PPN is involved in the initiation of locomotion and regulation of locomotor patterns, in addition to its capability of controlling postural muscle tone via projections to the pontomedullary reticular formation (Garcia-Rill, 1991; Takakusaki et al., 2003).

Based on findings described above, dysfunction of the PPN may disturb various movements and state of vigilance. Kojima et al. (1997) demonstrated that a kainic acid-induced lesion of the PPN produced hemiparkinsonism and suggested that dysfunction of the ascending projections from the PPN to the basal ganglia nuclei might underlie the pathophysiology of parkinsonism. It has been also supposed that dysfunction of the descending projections from the PPN results in gait failure (Garcia-Rill, 1986; Garcia-Rill et al., 1983; Pahapill and Lozano, 2000; Takakusaki et al., 2003) and muscular rigidity (Takakusaki et al., 2003) of parkinsonism. Moreover, a damage of the PPN may be involved in various types of sleep disturbance including REM sleep behavioral disorders (Rye et al., 1999).

References

Armstrong, D.A., Saper, C.B., Levey, A.I., Winer, B.H., Terry, R.D., 1983. Distribution of cholinergic neurons in the rat brain demonstrated by the immunohistochemical localization of choline acethyltransferase. J Comp Neurol. 216, 53-68.

Armstrong, D.M., 1986. Supraspinal contribution to the initiation and control of locomotion in the cat. Prog. Neurobiol. 26, 273-361.

Berman, A.L., 1968. The brain stem of the cat: cytoarchitectonic atlas with stereotaxic coordinates. Madison: University of Winsconsin Press.

Burke, R.E., 1968. Firing patterns of gastrocnemius motor units in the decerebrate cat. J. Physiol. 196, 631-654.

Carlton, S.M., Leichnetz, G.R., Young, E.G., Mayer, D.J., 1983. Supramedullary afferents of the nucleus raphe magnus in the rat: a study using the transcannula HRP gel and autoradiographic techniques. J. Comp. Neurol. 214, 43-58.

Chase, M.H., Morales, F.R., 1990. The atonia and myoclonia of active (REM) sleep. Ann Rev Psychol. 41, 557–584.

Chase, M.H., Morales, F.R., Boxer, P.A., Fung, S.J., Soja, P.J., 1986. Effect of stimulation of the nucleus reticularis gigantocellularis on the membrane potential of cat lumbar motoneurons during sleep and wakefulness. Brain Res. 386, 237–244.

Clements, J.R., Toth, D.D., Highfield, D.A., Grant, S.J., 1991. Glutamate-like immunoreactivity is present within cholinergic neurons in the laterodorsal tegmental and pedunculopontine nuclei. Adv Exp Med Biol. 295, 127-142.

Crone, C., Hultborn, H., Kiehn, O., Mazieres, L., Wigström H., 1988. Maintained changes in motoneuronal excitability by short-lasting synaptic inputs in the decerebrate cat. J. Physiol. 405, 321-343.

Datta, S., 2002. Evidence that REM sleep is controlled by the activation of brain stem pedunculopontine tegmental kainate receptor. J Neurophysiol. 87, 1790–1978.

Datta, S., Siwek, D.F., 2002. Single cell activity patterns of pedunculopontine tegmentum neurons across the sleep-wake cycle in the freely moving rats. J Neurosci Res. 15, 611-621.

Eccles R.M. and Lundberg A., 1958. Integrative patterns of Ia synaptic actions on motoneurones of hip and knee muscles. J. Physiol. 144, 271-298.

Fung, S.J., Barnes, C.D., 1981. Evidence of facilitatory coerulospinal action in lumbar motoneurons of cats. Brain Res. 261, 299-311.

Fung, S.J., Boxer, P.A., Morales, F.R., Chase, M.H., 1982. Hyperpolarizing membrane responses induced in lumbar motoneurons by stimulation of the nucleus reticularis pontis oralis during active sleep. Brain Res. 248, 267–273.

Gallager, D.W., Pert, A., 1978. Afferents to brain stem nuclei (brain stem raphe, nucleus reticularis pontis caudalis and nucleus gigantocellularis) in the rat as demonstrated by microiontophoretically applied horseradish peroxidase. Brain Res. 144, 257-275.

Garcia-Rill, E., 1986. The basal ganglia and the locomotor regions. Brain Res. 396, 47-63.

Garcia-Rill, E., 1991. The pedunculopontine nucleus. Prog. Neurobiol. 36: 363- 389.

Garcia-Rill, E., Houser, C.R., Skinner, R.D., Smith, W., Woodward, D.J., 1987. Locomotion-inducing sites in the vicinity of the pedunculopontine nucleus. Brain Res Bull. 18, 731-738.

Garcia-Rill, E., Skinner, R.D., Jackson, M.B., Smith, M.M., 1983. Connections of the mesencephalic locomotor region (MLR) I. Substantia nigra afferents. Brain Res Bull. 10, 57-62.

Garcia-Rill, E., Reese, N.B., Skinner, R.D., 1996. Arousal and locomotion: from schizophrenia to narcolepsy. Prog. Brain Res. 107, 417-434.

Glenn, L. L., Dement, W. C., 1981a. Membrane potential, synaptic activity, and excitability of hindlimb motoneurons during wakefulness and sleep. J Neurophysiol. 46, 839-854.

Glenn, L. L., Dement, W. C., 1981b. Membrane resistance and rheobase of hindlimb motoneurons during wakefulness and sleep. J Neurophysiol. 46, 1076-1088.

Glenn, L. L., Dement, W. C., 1981c. Group I excitatory and inhibitory potentials in hindlimb motoneurons during wakefulness and sleep. J Neurophysiol. 46, 1089-1101.

Grillner, S., Georgopoulos, A.P., Jordan L.M., 1997. Selection and initiation of motor behavior. In: Stein, P.S.G., Grillner, S., Selverson, A.I., Stuart, D.G. (Eds.), Neurons, Networks, and Motor Behavior, MIT Press, pp.3-19.

Habaguchi, T., Takakusaki, K., Saitoh, K., Sugimoto, J., Sakamoto, T., 2002. Medullary reticulospinal tract mediating the generalized motor inhibition in cats: II. Functional organization within the medullary reticular formation with respect to postsynaptic inhibition of forelimb and hindlimb motoneurons. Neuroscience 113, 65-77.

Henneman, E., Somjen, G., Carpenter, D., 1965. Functional significance of cell size in spinal motoneurons. J. Neurophysiol. 560-580.

Honda, T., Semba, K., 1994. Serotoergic synaptic input to cholinergic neurons in the rat mesopontine tegmentum. Brain Res. 647, 299-306.

Homma, Y., Skinner, R.D., Garcia-Rill, E., 2002. Effects of pedunculopontine nucleus (PPN) stimulation on caudal pontine reticular formation (PnC) neurons in vitro. J Neurophysiol. 87, 3033-3047.

Hounsgaard, J., Hultborn, H., Jespersen, B., Kiehn, O., 1984. Intrinsic Membrane properties causing a bistable behaviour of α-motoneurones. Exp. Brain Res. 55, 391-394.

Inglis, W.L., Winn, P., 1995. The pedunculopontine tegmental nucleus: where the striatum meets the reticular formation. Prog Neurobiol. 47, 1–29.

Jankowska, E., Lund, S., Lundberg, A., Pompeiano, O., 1968. Inhibitory effects evoked by through ventral reticulospinal pathways. Arch Ital Biol. 106, 124-140.

Jankowska, E., Roberts, W.J., 1972. Synaptic actions of single interneurones mediating reciprocal Ia inhibition of motoneurones. J Physiol. 222, 623-642.

Jones, B.E., 1991. Paradoxical sleep and its chemical/structural substrates in the brain. Neuroscience. 40, 637–656.

Katayama, Y., DeWitt, D.S., Becker, D.P., Hayes, R.L., 1984. Behavioral evidence for a cholinoceptive pontine inhibitory area: descending control of spinal motor output and sensory input. Brain Res. 296, 241-262.

Katz, B., Miledi, R., 1963. A study of spontaneous miniature potentials in spinal motoneurones. J Physiol. 168, 389-422.

Kernell, D., 1966. Input resistance, electrical excitability, and size of ventral horn cells in cat spinal cord. Science 152, 1637-1640.

Kernell, D., Zwaagstra, B., 1981. Input conductance, axonal conduction velocity and cell size among hindlimb motoneurones of the cat. Brain Res. 204, 311-326.

Kojima. J., Yamaji. Y., Matsumura. M., Nambu. A., Inase. M., Tokuno. H., Takada. M., Imai. H., 1997. Excitotoxic lesions of the pedunculopontine tegmental nucleus produce contralateral hemiparkinsonism in the monkey. Neurosci Lett. 226, 111-114.

Kosaka, T., Tauchi, M., Dahl, J., 1988. Cholinergic neurons containing GABA-like and/or glutamic acid decarboxylase-like immunoreactivities in various brain regions of the rat. Expl Brain Res. 70, 605–617.

Koyama Y, Sakai K., 2000. Modulation of presumed cholinergic mesopontine tegmental neurons by acetylcholine and monoamines applied iontophoretically in unanesthetized cats. Neuroscience 96, 723-733.

Lai, Y.Y., Kodama, T., Siegel, J.M., 2001.Changes in monoamine release in the ventral horn and hypoglossal nucleus linked to pontine inhibition of muscle tone: an in vivo microdialysis study. J. Neurosci. 21, 7384-7391.

Lai, Y.Y., Siegel, J.M., 1988. Medullary regions mediating atonia. J. Neurosci. 8, 4790-4796.

Lai, Y.Y., Siegel, J.M., 1990. Muscle tone suppression and stepping produced by stimulation of midbrain and rostral pontine reticular formation. J Neurosci. 10, 2727–2734.

Lai, Y.Y., Clements, J.R., Siegel, J.M., 1993. Glutamatergic and cholinergic projections to the pontine inhibitory area identified with horseradish peroxidase retrograde transport and immunohistochemistry. J Comp Neurol. 336, 321–330.

Leonald, C.S., Llinás, R., 1994. Serotonergic and cholinergic inhibition of mesopontine cholinergic neurons controlling REM sleep; an in vitro electrophysiological study. Neuroscience 59, 309-330.

Llinás, R., Terzuolo, C. A., 1964. Mechanisms of supraspinal actions upon spinal cord activities: Reticular inhibitory mechanisms on alpha-extensor motoneurons. J Neurophysiol. 27, 579-591.

Llinás, R., Terzuolo, C. A., 1965. Mechanisms of supraspinal actions upon spinal cord activities: Reticular inhibitory mechanisms upon flexor motoneurons. J Neurophysiol. 28, 413-422.

Magoun, H.W., Rhines, R., 1946. An inhibitory mechanisms in the bulbar reticular formation. J Neurophysiol. 9, 165-171.

Matsumura, M., Kojima, J., 2001. The role of the pedunculopontine tegmental nucleus in experimental parkinsonism in primates. Stereotact. Funct. Neurosurg. 77: 108-115.

Matsumura, M., Watanabe, K., Ohye, C., 1997. Single-unit activity in the primate nucleus tegmenti pedunculopontinus related to voluntary arm movement.

Neurosci Res. 28: 155-165.

McCormick, D.A., Bal, T., 1997. Sleep and arousal: thalamocortical mechanisms. Annu Rev Neurosci. 20, 185-215.

Mendell, L.M., Henneman, E., 1971. Terminals of single Ia fibers; location, density and distribution within a pool of 300 homonymous motoneurons. J Neurophysiol. 34, 171-187.

Mitani, A., Ito, K., Hallanger, A.E., Wainer, B.H., Kataoka, K., McCarley, R.W., 1988. Cholinergic projections from the laterodorsal and pedunculopontine tegmental nuclei to the pontine giganotocellular tegmental field in the cat. Brain Res. 451, 397–402.

Mogensen, G.J., Brudzynski, S.M., Wu, M., Yang, C.R., Yim, C.C.Y., 1993. From motivation to action: A review of dopaminergic regulation of limbic-nucleus accumbens-ventral pallidum-pedunculopontine nucleus circuits involved in limbic-motor integration. In: Kalivas, P.W. (Ed.), Limbic Motor Circuit and Neuropsychiatry, Boca Raton, FL: CRC, pp193-236.

Moon-Edley, S., Graybiel, A.M., 1983. The afferent and efferent connections of the feline nucleus tegmenti pedunculopontinus, pars compacta. J.Comp. Neurol. 217, 187-215.

Morales, F.R., Chase, M.H., 1978. Intracellular recording of lumbar motoneuron membrane potential during sleep and wakefulness. Expl Neurol. 62, 821-827.

Morales, F.R., Engelhardt, J., Soja ,P. J., Pereda, A.E., Chase, M.H., 1987. Motoneuron properties during motor inhibition produced by microinjection of carbachol into the pontine reticular formation of the decerebrate cat. J Neurophysiol. 57, 1118–1128.

Mori, S., 1987. Integration of posture and locomotion in acute decerebrate cats and in awake, free moving cats. Prog. Neurobiol. 28, 161-196.

Ottersen, O., Storm-Mathisen, J., 1984. Glutamate- and GABA containing neurons in the mouse and rat brain, as demonstrated with a new immunohistochemical technique. J Comp Neurol. 229, 374–392.

Pahapill P.A., Lozano A.M., 2000. The pedunculopontine nucleus and Parkinson's disease. Brain, 123, 1767-1783.

Reese, N.B., Garcia-Rill, E., Skinner, R.D., 1995. The pedunculopontine nucleus--auditory input, arousal and pathophysiology. Prog Neurobiol. 47, 105-133.

Rye, D.B., 1997. Contributions of the pedunculopontine region to normal and altered REM sleep. Sleep. 20, 757–88.

Rye, B.D., Saper, C.B., Lee, H.J., Wainer, B.H., 1987. Pedunculopontine tegmental nucleus of the rat: cytoarchitecture, cytochemistry, and some extrapyramidal connections of the mesopontine tegmentum. J Comp Neurol. 259, 483–528.

Sakai, K., Koyama, Y., 1996. Are there cholinergic and non-cholinergic paradoxical sleep-on neurones in the pons? Neuroreport. 7, 2449-2453.

Sakai, M., Matsunaga, M., Kubota, A., Yamanishi, Y., Nishizawa, Y., 2000. Reduction in excessive muscle tone by selective depletion of serotonin in intercollicularly decerebrated rats. Brain Res. 860, 104-111.

Schwindt, P. C., Crill, W. E., 1980. Role of a persistent inward current in motoneuron bursting during spinal seizure. J. Neurophysiol. 43, 1296-1318.

Semba, K., 1993. Aminergic and cholinergic afferents to REM sleep induction regions of the pontine reticular formation in the rat. J Comp Neurol. 330, 543-556.

Semba, K., Fibiger, H.C., 1992. Afferent connections of the laterodorsal and the pedunculopontine tegmental nuclei in the rat: a retro- and anterograde transport and immunohistochemical study. J Comp Neurol. 323, 387–410.

Shiromani, P.J., Lai, Y.Y., Siegel, J.M., 1990. Descending projections from the dorsolateral pontine tegmentum to the paramedian reticular nucleus of the caudal medulla in the cat. Brain Res. 28, 224–228.

Skinner, R.D., Kinjo, N., Ishikawa, Y., Biedermann, J.A., Garcia-Rill, E., 1990. Locomotor projections from the pedunculopontine nucleus to the medioventral medulla. Neuroreport. 1, 207-210.

Snider, R.S., Niemer, W.T., 1961. A stereotaxic atlas of the cat brain. Chicago: University of Chicago Press.

Spann, B.M., Grofova, I., 1992. Cholinergic and non-cholinergic neurons in the rat pedunculopontine tegmental nucleus. Anat Embryol. 186, 215–227.

Steriade, M., 2001. Impact of network activities on neuronal properties in corticothalamic systems. J Neurophysiol. 86,1-39.

Steriade, M., Datta, S., Pare, D., Oakson, G., Curro Dossi, R.C., 1990a. Neuronal activities in brain-stem cholinergic nuclei related to tonic activation processes in thalamocortical systems. J Neurosci. 10, 2541-59

Steriade, M., Pare, D., Datta, S., Oakson, G., Curro Dossi, R., 1990b. Different cellular types in mesopontine cholinergic nuclei related to ponto-geniculo-occipital waves. J Neurosci. 10, 2560–2579.

Sugaya, K., Mori, S., Tsuchida, S., 1988. Input and output neuronal structures of the pontine micturition center. Part I. Mainly input neuronal structures. Jpn. J. Urol. 79, 1210-1218.

Takakusaki, K., Habaguchi, T., Nagaoka, T., Sakamoto, T., 1997a. Stimulus effects of the pedunculopontine tegmental nucleus (PPN) on hindlimb motoneurons in cats. Soc Neurosci Abstr, 23, p 762.

Takakusaki K, Habaguchi T, Ohtinata-Sugimoto J, Saitoh K, Sakamoto T. 2003. Basal ganglia efferents to the brainstem centers controlling postural muscle tone and locomotion; A new concept for understanding motor disorders in basal ganglia dysfunction. Neuroscience. 119, 293-308.

Takakusaki, K., Kohyama, J., Matsuyama, K., Mori, S., 2001. Medullary reticulospinal tract mediating the generalized motor inhibition in cats: parallel inhibitory

mechanisms acting on motoneurons and on interneuronal transmission in reflex pathways. Neuroscience. 103, 511–527.

Takakusaki, K., Kohyama, J., Matsuyama, K., Mori, S., 1993a. Synaptic mechanisms acting on lumbar motoneurons during postural augmentation induced by serotonin injection into the rostral pontine reticular formation in decerebrate cats. Expl Brain Res. 93, 471-82.

Takakusaki, K., Matsuyama, K., Kobayashi, Y., Kohyama, J., Mori, S., 1993b. Pontine microinjection of carbachol and critical zone for inducing postural atonia in reflexively standing decerebrate cats. Neurosci Lett 153, 185-188.

Takakusaki, K., Saitoh, K., Ohinata-Sugimoto, J., Satoh, E., 2002. Evidence of the basal ganglia control of muscular atonia associating with rapid eye movements (REM) in cats: Possible role of the basal ganglia in the generation of REM sleep. Soc Neurosci Abstr. 28, 361.4.

Takakusaki, K., Shimoda, N., Matsuyama, K., Mori, S., 1994. Discharge properties of medullary reticulospinal neurons during postural changes induced by intrapontine injections of carbachol, atropine and serotonin, and their functional linkages to hindlimb motoneurons in cats. Expl Brain Res. 99, 361–374.

Takakusaki, K., Shiroyama, T., Yamamoto, T., Kitai, S.T., 1996. Cholinergic and non-cholinergic tegmental pedunculopontine projection neurons in rats revealed by intracellular labeling. J Comp Neurol. 371, 345–361.

Talley, E.M., Sadr, N.N., Bayliss, D.A., 1997. Postnatal development of serotonergic innervation, 5-HT1A receptor expression, and 5-HT responses in rat motoneurons. J Neurosci. 17, 4473-85.

Vanni-Mercier, G., Sakai, K., Lin, J.S., Jouvet, M., 1989. Mapping of cholinoceptive brainstem structures responsible for the generation of paradoxical sleep in the cat. Arch Ital Biol. 127, 133-64.

Vincent, S.R., Satoh, K., Armstrong, D.M., Fibiger, H.C., 1983. Substance P in the ascending cholinergic reticular system. Nature. 306, 688-691.

White, S.R., Fung, S.J., 1989. Serotonin depolarizes cat spinal motoneurons in situ and decreases motoneuron afterhyperpolarizing potentials. Brain Res. 502, 205-213.

Yamamoto, K., Mamelak, A.N., Quattrochi, J.J., Hobson, J.A., 1990. A cholinoceptive desynchronized sleep induction zone in the anterodorsal pontine tegmentum: locus of the sensitive region. Neuroscience 39, 279-293.

Acknowledgments

This study was supported by the Japanese Grants-in-Aid for Priority Areas (A), RISTEX of JST (Japan Science and Technology Agency) and Uehara memorial foundation.

Figure legends

Figure 1. Effective electrical stimulus sites in the mesopontine tegmentum for muscular atonia

A. (a) Microphotographic presentation of the stimulus site and cholinergic neurons labeled by ChAT immunohistochemistry. (b) Higher magnification of the area enclosed by a square in (a). Arrows indicate the stimulus site. B. (a) Effective sites are shown on coronal planes at the level of P 1.5 (left) and P 2.0 (right). (b) Effective sites are shown on parasagittal planes at the level of LR 4.0 (left) and LR 4.5 (right). CNF, cuneiform nucleus; IC, inferior colliculus, LR; left-right; NRPo; nucleus reticularis pontis oralis, P; posterior, PPN; pedunculopontine tegmental nucleus; SC, superior colliculus; SCP, superior cerebellar peduncle.

Figure 2. Mesopontine stimulus effects on an LG-S motoneuron

A. Changes in membrane potentials of an LG-S motoneuron. (a) Stimulation of the CNF induced a membrane depolarization which was followed by membrane oscillations with a frequency of approximately 1 Hz. (b) Stimulation of the dorsal part of the PPN hyperpolarized the membrane potentials. The membrane hyperpolarization was followed by membrane oscillation with a frequency of approximately 1.5 Hz. (c) Stimulation of the ventral part of the PPN induced membrane hyperpolarization which persisted even after termination of the stimulation. A line beneath each recording indicates the period of stimulation with an intensity of 30 μA and a frequency of 50 Hz. These recordings were induced by stimuli applied to each site in B. The dashed line in each recording indicates the threshold of this motoneuron. B. Stimulus sites in the mesopontine tegmentum on a coronal plane at P 2.0. Stimuli were applied to P2.0, L4.0, and H -1.0 for (a); P2.0, L4.0, and H -2.0 for (b); and P2.0, L4.0, and H -3.0 for (c). C. Orthodromic (a) and antidromic (b) action potentials induced by stimulating a nerve innervating the LG-S muscles. The upper and lower traces are intracellular activity and

cord dorsum potentials, respectively. CS, centralis superior; P, pyramidal tract; RD, raphe dorsalis.

Figure 3. Changes in membrane potentials following the PPN stimulation
A. Intracellular recording of an LG-S motoneuron. (a) Stimulation of the PPN with an intensity of 30 μA gradually decreased the firing rate and hyperpolarized the membrane potentials approximately 8 mV. (b) Stimulation of the PPN with an intensity of 40 μA immediately stopped spontaneous firing, and this was followed by a membrane hyperpolarization of 12 mV. The dashed line in each recording indicates the threshold potential (-55 mV) of this LG-S motoneuron. B and C. The PPN stimulation with an intensity of 40 μA in the same animal induced a membrane hyperpolarization in Q (B) and PBSt (C) motoneurons. The dashed lines in B (-64 mV) and C (-60 mV) indicate the prestimulus membrane potential levels. D. The degree of membrane hyperpolarization of 72 hindlimb motoneurons. (a) PPN stimulation hyperpolarized 2–9 mV (mean $\pm$ standard deviation; 5.3 $\pm$ 1.6 mV) in 60 motoneurons without spontaneous firing before stimulation (silent cells). (b) PPN stimulation hyperpolarized 8–12 mV (mean $\pm$ standard deviation; 10.0 $\pm$ 1.5 mV) in 12 motoneurons with spontaneous firing before stimulation (firing cells). E. The relationship between PPN-induced membrane hyperpolarization and membrane potentials before stimulation in 60 silent cells. There was a significant correlation between them. PPN stimuli with parameters of 40 μA, 50 Hz, and a duration of 5–10 seconds, were employed for the results in D and E.

Figure 4. PPN-induced changes in the firing capability of hindlimb motoneurons
In A–C, left panels are changes in membrane potentials of LG-S (A), PBSt (B) and LG-S (C) motoneurons following the PPN stimulation with intensities of 30 μA and 50 μA. Membrane potential levels just before the generation of each action potential, which was evoked at every 1 second, were measured and plotted by either open and

filled circles. At the membrane potential levels denoted by filled circles, action potentials were blocked by PPN stimulation. However, the stimulation did not block the generation of action potentials at the membrane potential levels which were denoted by open circles. Right panels are superimposition of action potentials induced by orthodromic conduction (A), antidromic conduction (B) and intracellular injection of a constant depolarizing current (C). In each motoneuron, action potentials in (a)-(d) were recorded at the periods indicated by (a)-(d) in the left panels. In A, the firing capability of orthodromic spikes was reduced by PPN stimulation with 30 μA, and completely removed by stimulation with 50 μA. In B, PPN stimulation with 30 μA increased a fragmentation of the initial segment-somatodendric (IS-SD) spikes (IS-SD delay), and stronger stimuli (50 μA) finally abolished the SD spikes (IS-SD block). In C, constant-current pulses of 15 nA with a duration of 200 μs were used to evoke action potentials. The firing capability and the membrane potential of each motoneuron were gradually returned after termination of the PPN stimulation.

Figure 5 Changes in the input resistance of hindlimb motoneurons
A. The upper trace indicates anodal and cathodal pairs of pulses (± 4 nA, 50 ms) pulses and the lower trace indicates the intracellular membrane potentials of a PBSt motoneuron. These pulses were delivered into a PBSt motoneuron through a micropipette at intervals of 1 second. B. (a) – (c) Each trace is a superimposition of membrane potentials in response to the injecting currents before (a), during (b) and after (c) PPN stimulation. PPN stimulation hyperpolarized the membrane potential together with a decrease in input resistance. Traces beneath the records (a) and (b) are anodal and cathodal pairs of pulses (± 4 nA, 50 ms) pulses and extracellular potentials in response to the current. C. Time course of the changes in input resistance (open circles) and membrane potential (filled circles) of the PBSt motoneuron and a Q motoneuron.

Figure 6. Changes in the membrane properties of motoneurons following the PPN stimulation

A. Baseline membrane properties of hindlimb motoneurons. (a) There was an inverse correlation between the input resistance and conduction velocity. (b) The membrane potential was correlated with the input resistance. B. Changes in membrane properties during PPN stimulation. (a) PPN-induced membrane hyperpolarization was inversely correlated with the conduction velocity. (b) There was a correlation between the PPN-induced membrane hyperpolarization and the PPN-induced decrease in input resistance.

Figure 7. Changes in monosynaptic Ia EPSPs induced by PPN stimulation

A. Changes in Ia EPSPs in an MG motoneuron before (a), during (b) and after (c) PPN stimulation. The upper and lower traces are intracellular potentials and cord dorsum potentials, respectively. PPN stimulation greatly reduced the amplitude of Ia EPSPs together with the membrane hyperpolarization (b). After PPN stimulation, the amplitude returned or was increased (c). B. Changes in Ia EPSPs and input resistance in a PBSt motoneuron before (a), during (b) and after (c) PPN stimulation. The upper sets of recordings are intracellular potentials and cord dorsum potentials, respectively. The lower sets of recordings are membrane potentials and anodal pulses (10 nA, 100 ms duration), respectively. Despite the large reduction of the Ia EPSPs (31% of the control) during PPN stimulation, the input resistance was reduced to 65.6% of the control (b). In A and B, each recording was the average of 8 sweeps. C. A semilogarithmic plot of the time course of decay for the Ia EPSPs in an MG (a) and PBSt (b) motoneuron. A decrease was observed in the peak amplitude, and an increase in the rate of decay of the Ia EPSPs during PPN stimulation (filled circles), compared to before (hatched circles), and after the stimulation (open circles).

Figure 8. The effects of intracellular injection of chloride ions

A. Changes in Ia IPSPs in an LG-S motoneuron. (a) Stimulating the Ia afferents from the TA muscles induced monosynaptic Ia IPSPs. (b) The amplitude of the Ia EPSPs was greatly reduced 20 minutes after the chloride injection. (c) The polarity of the EPSPs was reversed 35 minutes after the chloride injection. B. Changes in membrane potentials of the LG-S motoneuron induced by PPN stimulation. (a) PPN stimulation caused the spontaneous firing to cease and hyperpolarized the membrane potentials. (b) After 22 minutes the membrane potential level was not changed during the PPN stimulation, but was hyperpolarized after termination of the stimulation. (c) After 38 minutes, PPN stimulation depolarized the membrane. However, the motoneuron was gradually hyperpolarized after the stimulation. C. Changes in the amplitude of Ia IPSPs and the degree of PPN-induced membrane hyperpolarization following chloride ion injections in Q (open squares), PBSt (filled circles) and LG-S (open squares) motoneurons. In an LG-S motoneuron, each value in (a) – (c) was obtained from (a) – (c) in A and B.

Table 1. Changes in electrophysiological membrane properties (A) and shape parameters of Ia EPSPs following the stimulation of the PPN.

A Membrane properties

	Cell #	Control	PPN stim.	After
Membrane potentials (mV)	n=72	-60.7 ± 4.2	-66.7 ± 4.2*	-64.8 ± 3.8*
(changes mV)			(6.0 ± 2.3)	(4.1 ± 2.3)
Input resistance (MΩ)	n=14	1.38 ± 0.51	0.89 ± 0.37*	1.39 ± 0.58
(relative changes; %)			(64.5 ± 6.7)	(101.3 ± 4.9)

B Shape parameters of Ia EPSPs

	Cell #	Control	PPN stim.	After
Peak voltage (mV)	n=14	4.37 ± 2.61	2.39 ± 1.47*	4.46 ± 2.79
(relative changes; %)			(56.9 ± 13.4)	(102.1 ± 3.7)
Times to peak (ms)	n=14	1.26 ± 0.23	0.94 ± 0.20*	1.30 ± 0.20
(relative changes; %)			(75.3 ± 13.4)	(103.1 ± 4.9)
Half width (ms)	n=14	4.71 ± 1.26	3.31 ± 0.84*	4.86 ± 1.25
(relative changes; %)			(70.3 ± 11.1)	(103.2 ± 2.7)

* The values are different from those of control ($p<0.05$).

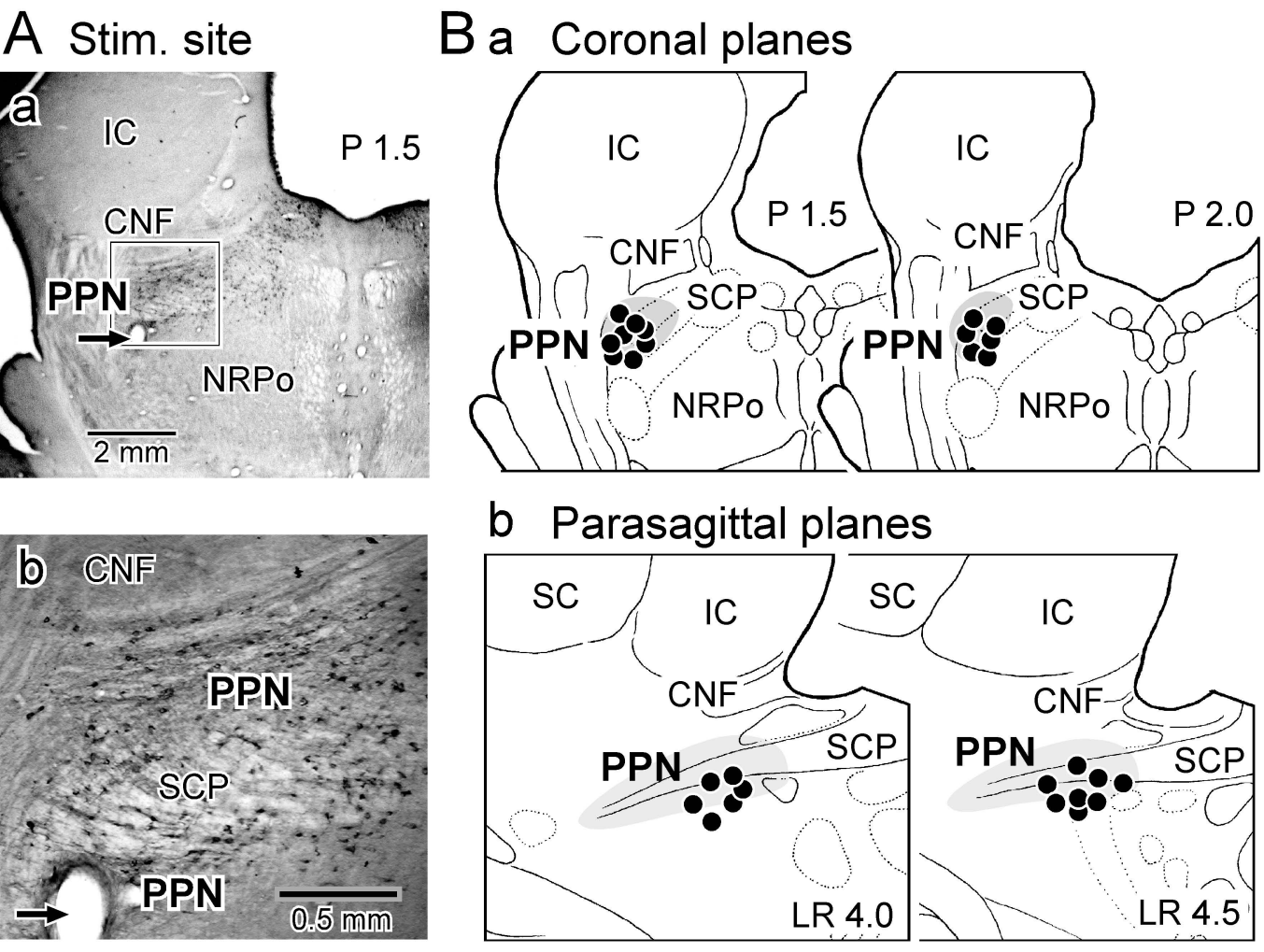
A Stim. site
a
IC
P 1.5
CNF
PPN
NRPo
2 mm
b
CNF
PPN
SCP
PPN
0.5 mm
B a Coronal planes
IC
P 1.5
CNF
SCP
PPN
NRPo
IC
P 2.0
CNF
SCP
PPN
NRPo
b Parasagittal planes
SC
IC
CNF
SCP
PPN
LR 4.0
SC
IC
CNF
SCP
PPN
LR 4.5

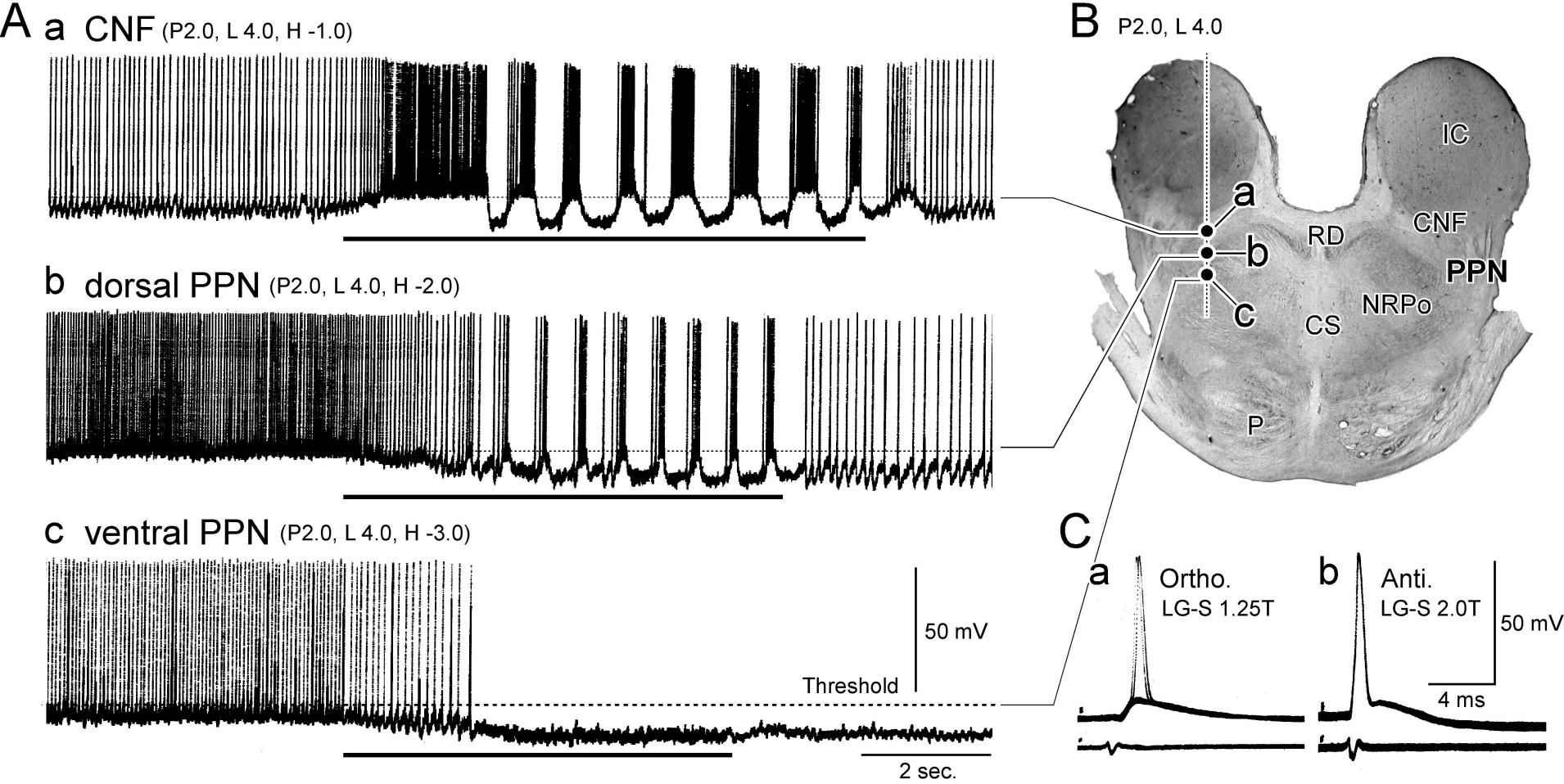
A
a CNF (P2.0, L 4.0, H -1.0)
b dorsal PPN (P2.0, L 4.0, H -2.0)
c ventral PPN (P2.0, L 4.0, H -3.0)
50 mV
Threshold
2 sec.
B
P2.0, L 4.0
IC
a
RD
CNF
b
PPN
NRPo
c
CS
P
C
a
Ortho.
LG-S 1.25T
b
Anti.
LG-S 2.0T
50 mV
4 ms

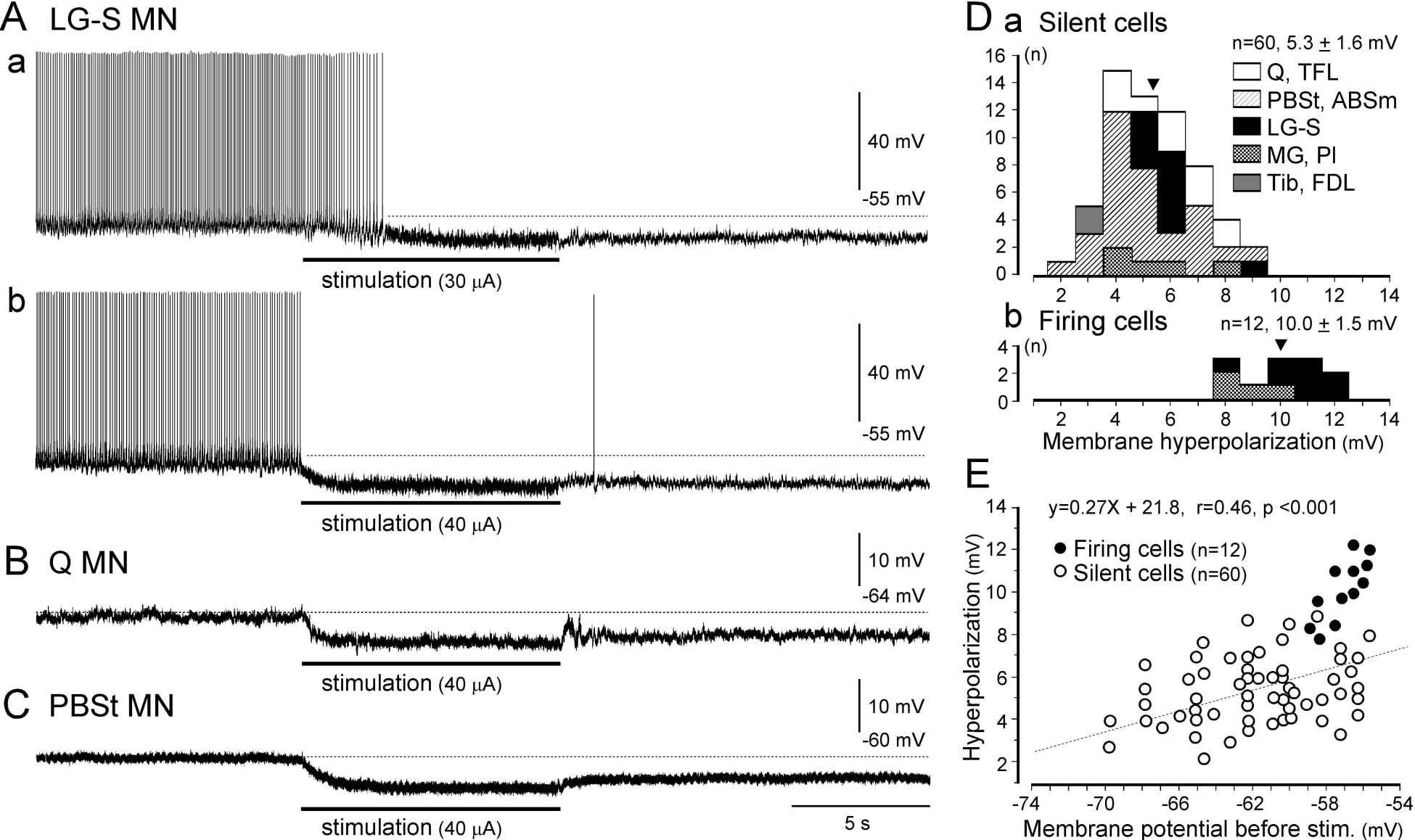
A LG-S MN
a
40 mV
-55 mV
stimulation (30 μA)
b
40 mV
-55 mV
stimulation (40 μA)
B Q MN
10 mV
-64 mV
stimulation (40 μA)
C PBSt MN
10 mV
-60 mV
stimulation (40 μA)
5 s
D a Silent cells
n=60, 5.3 ± 1.6 mV
(n)
Q, TFL
PBSt, ABSm
LG-S
MG, PI
Tib, FDL
b Firing cells
n=12, 10.0 ± 1.5 mV
Membrane hyperpolarization (mV)
E
y=0.27X + 21.8, r=0.46, p <0.001
Firing cells (n=12)
Silent cells (n=60)
Hyperpolarization (mV)
Membrane potential before stim. (mV)

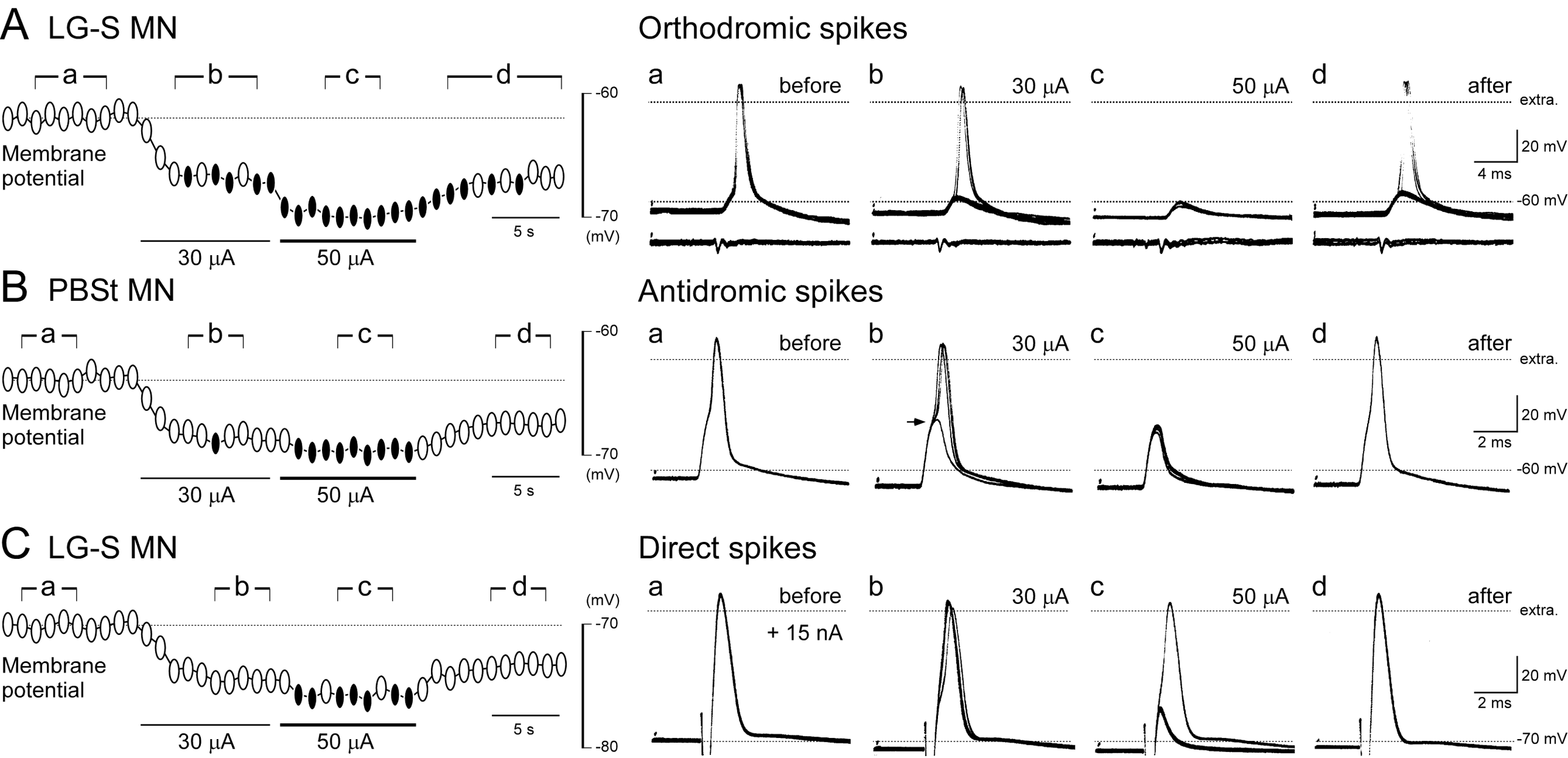
A LG-S MN
a
b
c
d
Membrane potential
-60
-70
(mV)
5 s
30 μA
50 μA
Orthodromic spikes
a
before
b
30 μA
c
50 μA
d
after
extra.
20 mV
4 ms
-60 mV
B PBSt MN
Antidromic spikes
2 ms
C LG-S MN
Direct spikes
+ 15 nA
-80
-70 mV

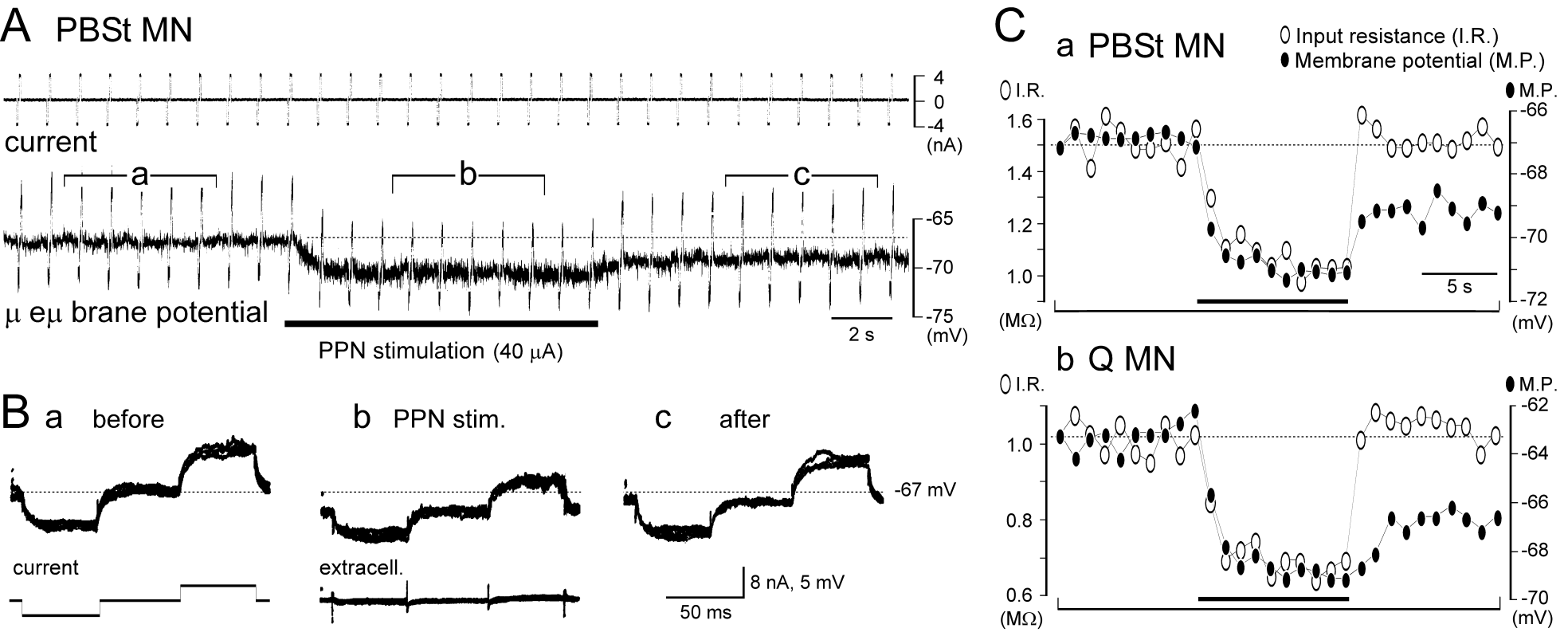
A PBSt MN
4
0
-4
(nA)
current
a
b
c
-65
-70
-75
(mV)
μ eμ brane potential
2 s
PPN stimulation (40 μA)
B a before
b PPN stim.
c after
-67 mV
current
extracell.
8 nA, 5 mV
50 ms
C
a PBSt MN
Input resistance (I.R.)
Membrane potential (M.P.)
I.R.
M.P.
1.6
1.4
1.2
1.0
-66
-68
-70
-72
5 s
(MΩ)
(mV)
b Q MN
I.R.
M.P.
1.0
0.8
0.6
-62
-64
-66
-68
-70
(MΩ)
(mV)

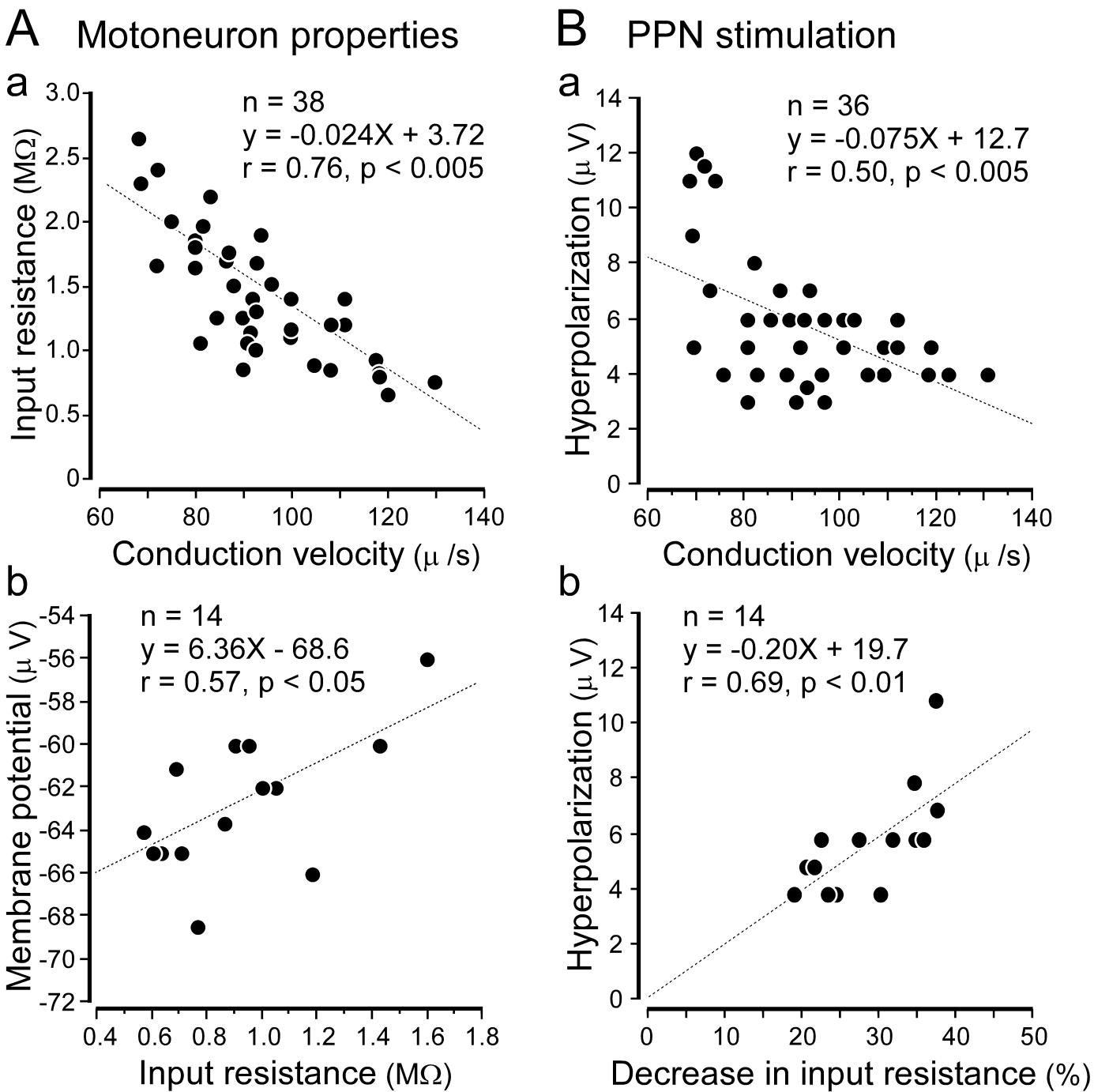
A
Motoneuron properties
a
n = 38
y = -0.024X + 3.72
r = 0.76, p < 0.005
Input resistance (MΩ)
Conduction velocity (μ /s)
b
n = 14
y = 6.36X - 68.6
r = 0.57, p < 0.05
Membrane potential (μ V)
Input resistance (MΩ)
B
PPN stimulation
a
n = 36
y = -0.075X + 12.7
r = 0.50, p < 0.005
Hyperpolarization (μ V)
Conduction velocity (μ /s)
b
n = 14
y = -0.20X + 19.7
r = 0.69, p < 0.01
Hyperpolarization (μ V)
Decrease in input resistance (%)

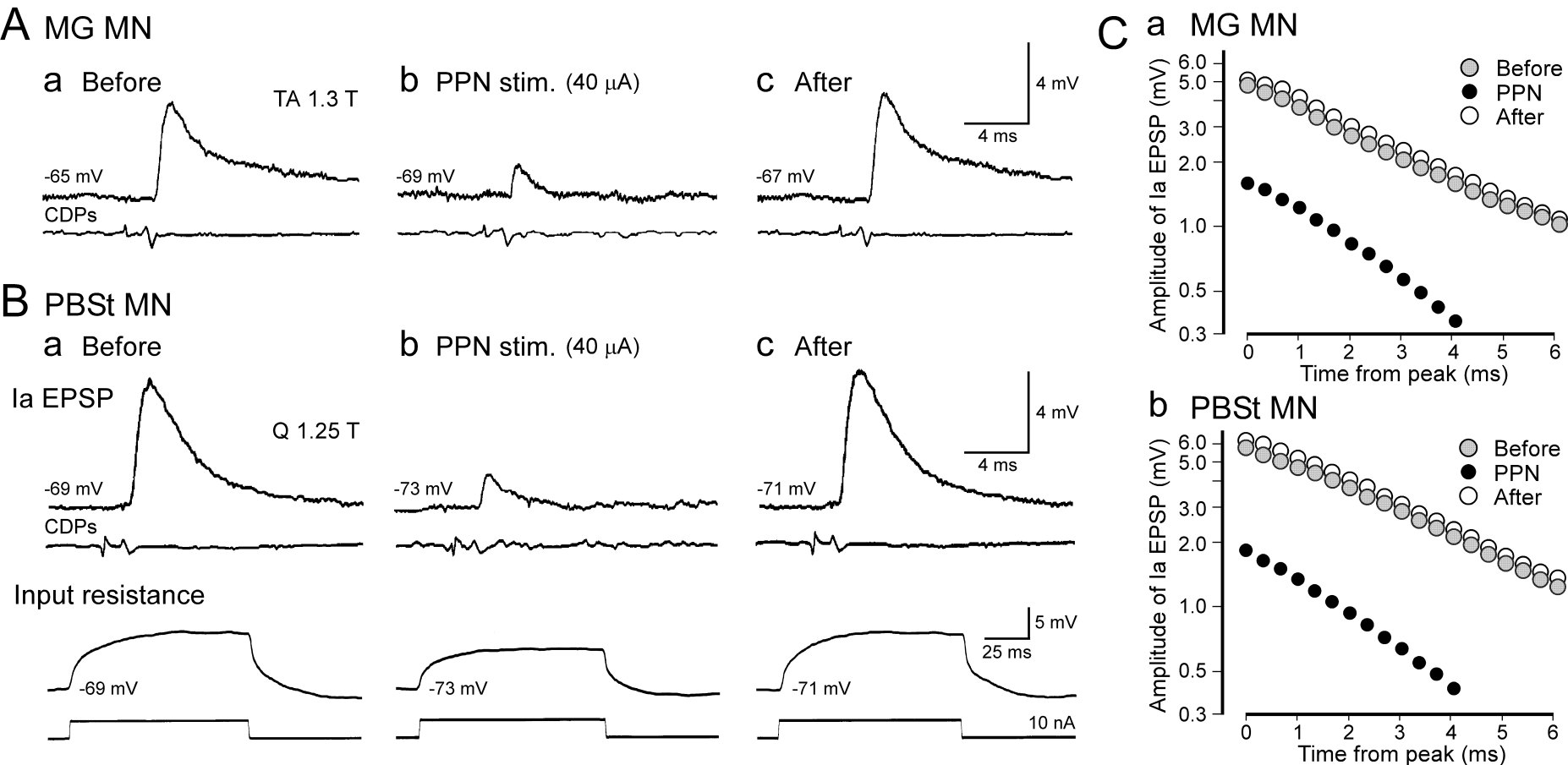
A MG MN
a Before
TA 1.3 T
-65 mV
CDPs
b PPN stim. (40 μA)
-69 mV
c After
-67 mV
4 mV
4 ms
B PBSt MN
a Before
Ia EPSP
Q 1.25 T
-69 mV
CDPs
b PPN stim. (40 μA)
-73 mV
c After
-71 mV
4 mV
4 ms
Input resistance
-69 mV
-73 mV
-71 mV
5 mV
25 ms
10 nA
C a MG MN
Amplitude of Ia EPSP (mV)
Time from peak (ms)
Before
PPN
After
b PBSt MN
Amplitude of Ia EPSP (mV)
Time from peak (ms)
Before
PPN
After

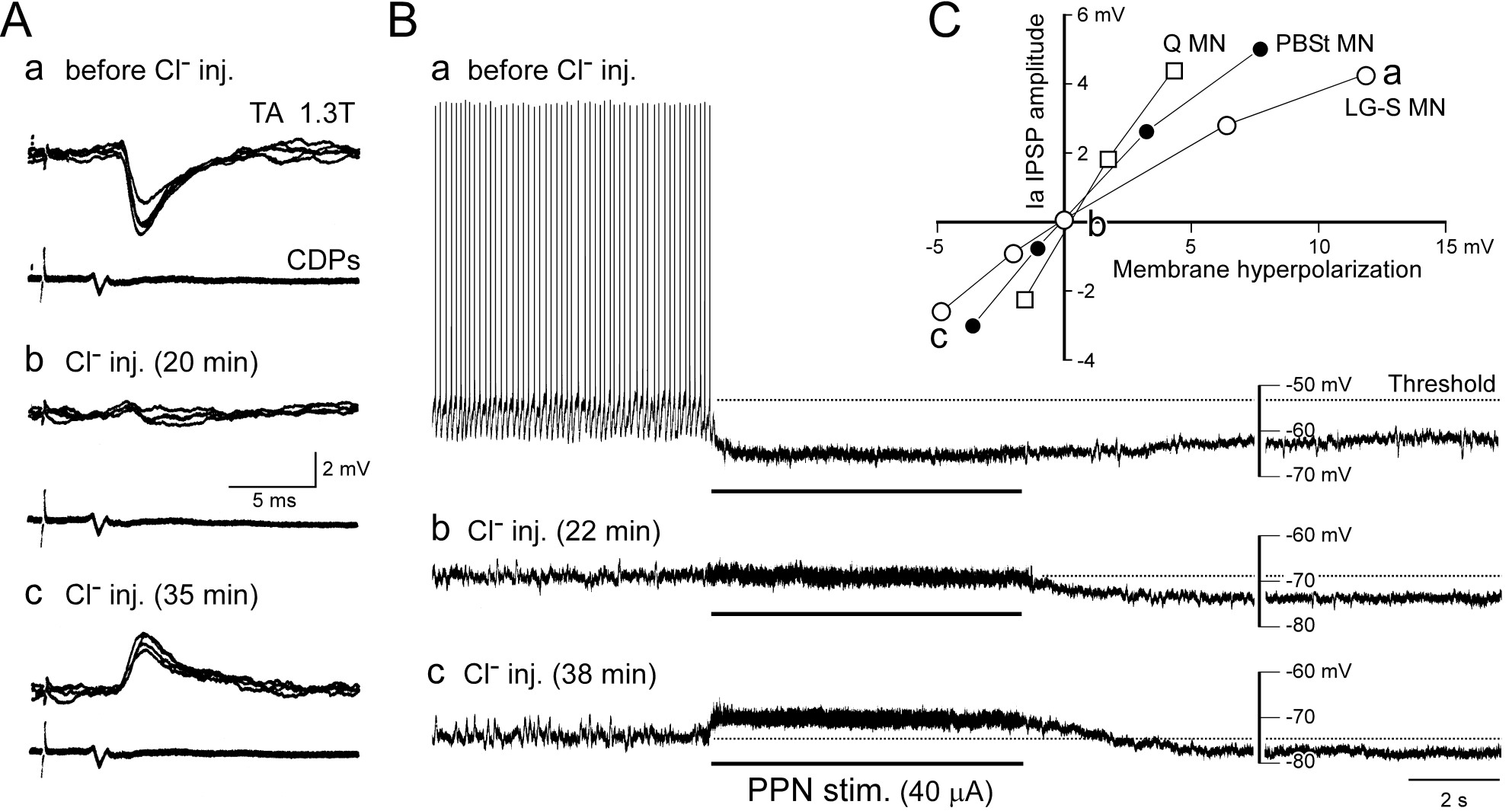
A
a before Cl⁻ inj.
TA 1.3T
CDPs
b Cl⁻ inj. (20 min)
2 mV
5 ms
c Cl⁻ inj. (35 min)
B
a before Cl⁻ inj.
-50 mV
Threshold
-60
-70 mV
b Cl⁻ inj. (22 min)
-60 mV
-70
-80
c Cl⁻ inj. (38 min)
-60 mV
-70
-80
PPN stim. (40 μA)
2 s
C
Ia IPSP amplitude
6 mV
4
2
-2
-4
-5
5
10
15 mV
Membrane hyperpolarization
Q MN
PBSt MN
LG-S MN
a
b
c